12

MR Angiography in Liver Disease

CONTENTS

12.1 Introduction

Recent developments in magnetic resonance (MR) scanner hardware and the advent of fast three dimensional (3D) gradient echo sequences have rapidly advanced the role of MR imaging for the evaluation of abdominal vasculature. Nowadays it is possible to accurately image both the arterial and venous vasculature of the abdomen and to acquire sufficient information to accurately detect and diagnose underlying pathologies of these vessels. In particular, depiction of anatomic variants of the arterial blood supply and demonstration of collateral circulation of the liver is easily performed non-invasively on contrast-enhanced MR angiography (CE MRA). The possibility to perform rapid time-resolved imaging permits evaluation of both the arterial and portal-venous systems in the same session, thereby rendering CE MRA a one-stop-shop for the work-up of patients with suspected vascular disease of the liver. The rapid improvements in CE MRA methodology permit accurate non-invasive evaluation of potential living donors and of patients scheduled for liver transplantation.

12.2 Technique

MRA does not require extensive patient preparation prior to the examination. Patients are not required to fast before the examination; on the contrary, high-caloric meals prior to the examination may increase the splanchnic flow, thereby improving the depiction of small branching arteries. On the other hand, physiological peristalsis may cause motion artifacts in some patients; this can be reduced by application of glucagon or N-butyl-scopalamine.

Imaging is usually performed with the patient in the supine position in the magnet. Typically, a body array surface coil that covers the abdomen is used. The arms should be elevated above the head in order to avoid aliasing artifacts. For accurate injection of contrast agent, an intravenous feed should be placed in the right antecubital vein. For most examinations the contrast agent and saline flush should be injected at a minimum flow rate of 2 ml/sec in order to achieve a sufficiently tight contrast agent bolus [25].

12.2.1 Time-of-Flight MRA

In order to achieve adequate signal in the vessels of interest, time-of-flight MR angiography (TOF MRA) generally requires the orthogonal acquisition of images. TOF MRA is therefore not suitable for depiction of the abdominal vasculature because of the typically tortuous course of the vessels. Although the proximal parts of the main abdominal branches in which most vascular pathologies are located may theoretically be assessed on TOF MRA, the long acquisition times for these sequences preclude the possibility of acquiring images in one breath-hold. Moreover, since flow in the aorta is perpendicular to that in the branching arteries, major artifacts which may mimic stenoses are common.

12.2.2 Phase-Contrast MRA

The abdominal vasculature may be evaluated with phase-contrast (PC) MRA using both two dimensional (2D) and 3D techniques [4, 14, 15, 21]. 2D PC MRA with electrocardiogram (ECG) or pulse triggering has been shown to provide functional information of the mesenteric vasculature [4, 14, 15, 21]. By segmenting the acquired phase with the cardiac cycle, quantitative measurements of flow velocity and volume may be acquired.

An important advantage of 3D PC MRA over 2D PC MRA is that images can be acquired in any plane [34]. However, due to the relatively long acquisition times, respiratory motion artifacts frequently impair the quality of the image. Moreover, image quality may be further reduced by ghost artifacts derived from inhomogeneous or turbulent flow during systole. Although this problem may be resolved by cardiac gating, this further increases the acquisition time without necessarily improving the image quality.

12.2.3 Contrast-Enhanced MRA

The acquisition of high quality images of the mesenteric vessels became feasible with the introduction of CE MRA [18, 26, 27]. Moreover, the technique permits the visualization of very small vessels that are not discernible using non-enhanced imaging techniques.

Imaging in the coronal plane permits evaluation of the aorta, splanchnic arteries and portal vein in one examination. A partition thickness of 3-5 mm is acceptable if zero padding is available for interpolation. In the absence of an interpolation algorithm, the slice thickness should be less than 3 mm. To evaluate stenotic disease of the celiac trunk or the proximal mesenteric arteries, imaging should be performed in the sagittal plane. Aliasing is not as severe for acquisitions in the sagittal plane, so it is possible to utilize a rectangular field-of-view with a high spatial resolution acquisition matrix (e.g. 512 x 256). If a slower MR system is used, it is advantageous to acquire images in the sagittal plane so that fewer sections or partitions are required to cover the aorta, celiac artery (CA), superior mesenteric artery (SMA), and inferior mesenteric artery (IMA). Imaging parameters should be adjusted to allow for image acquisition during breath-hold. Axial imaging may be useful if the primary goal is evaluation of the hepatic arteries, hepatic parenchyma or portal vein. However, one difficulty with the axial orientation is aliasing in the slice direction, which tends to be severe with the extremely short radio frequency (RF) pulses used in 3D CE MRA. To minimize aliasing, a coil should be used in which the cranial-dimension is only slightly larger than the caudal-dimension of the imaging volume. Fat saturation or chemically selective fat inversion pulses should also be considered. These will help minimize unwanted signal from pericardial and abdominal fat wrapping onto the image volume.

3D CE MRA datasets should be acquired before, during and after completion of intravenous contrast agent administration. Pre-contrast images should be checked to ensure that the imaging volume is positioned correctly. These images can also be used subsequently for digital subtraction to improve image contrast. Accurate timing of the contrast agent bolus is essential for arterial phase acquisitions. This can be achieved with automatic triggering (SmartPrep or Care Bolus), fluoroscopic triggering (Bolus Track) or by means of a test bolus to the mid-abdominal aorta. After arterial phase imaging, acquisition of a delayed image dataset is useful to show the portal-venous and hepatic venous anatomy. Arterial phase 3D CE MRA is best evaluated by first acquiring multiple overlapping maximum intensity projection (MIP) reconstructions in the coronal plane. Thereafter, reformations and subvolume MIP reconstructions can be prepared in perpendicular planes through each major abdominal aortic branch vessel, including the celiac trunk, and the SMA and IMA. It is also useful to assess the iliac arteries, especially the internal iliac arteries, as they may represent an important collateral pathway in patients with chronic mesenteric ischemia.

12.3 Imaging of the Arterial System

12.3.1 Normal Anatomy and Variants

The blood supply to the intra-abdominal organs derives from three major branches of the abdominal aorta: the celiac artery (CA), the SMA and the IMA. Although numerous anatomical variants exist, in the majority of cases CE MRA allows a detailed depiction of the typical and atypical vascular anatomy of the splanchnic vessels [2, 11, 17, 33]. Of principal interest for the arterial supply of the liver are the CA and the SMA, however, since collateral supply between the three major branches exists, all of these branches will be discussed (Fig. 1).

12.3.1.1 Celiac Artery (CA)

The CA is typically located at the level of the T12 to L1 vertebral body. It arises from the ventral part of the abdominal aorta and supplies the upper abdominal viscera. In about two thirds of patients the CA branches into the common hepatic artery, the splenic artery and the left gastric artery (Fig. 2). However, in the remaining one third of individuals, anatomical variants exist in which the common hepatic artery, the splenic artery and the left gastric artery arise from either the SMA or directly from the aorta.

The common hepatic artery divides into the proper hepatic artery and the gastroduodenal artery. In about 75% of cases the gastroduodenal artery thereafter branches into two further vessels; the right gastroepiploic artery and the superior pancreaticoduodenal artery. The superior pancreaticoduodenal artery forms an anastomosis with the inferior pancreaticoduodenal artery which derives from the SMA.

In about 50% of cases the proper hepatic artery divides into the left and right hepatic arteries. The remaining 50% of individuals show variants or accessory hepatic arteries. The main variants are shown in Fig. 3.

12.3.1.2 Superior Mesenteric Artery (SMA)

The SMA usually arises about 1 cm distal to the celiac artery at the anterior aspect of the aorta. In rare cases, a common single celio-mesenteric trunk is present. The first branch from the SMA is the inferior pancreaticoduodenal artery which forms an anastomosis with the superior pancreaticoduodenal artery deriving from the celiac artery. The jejunal and ileal branches arise from the proximal and left side of the SMA, forming multiple arcades. Right sided branches are the ileocolic artery, the right colic artery and the middle colic artery (Fig. 4).

A common variant is the origin of the right hepatic artery from the SMA or even the origin of the common hepatic artery from the SMA.

12.3.1.3 Inferior Mesenteric Artery (IMA)

The IMA arises from the abdominal aorta at approximately the level of the third lumbar vertebra. Compared to the other main abdominal branches

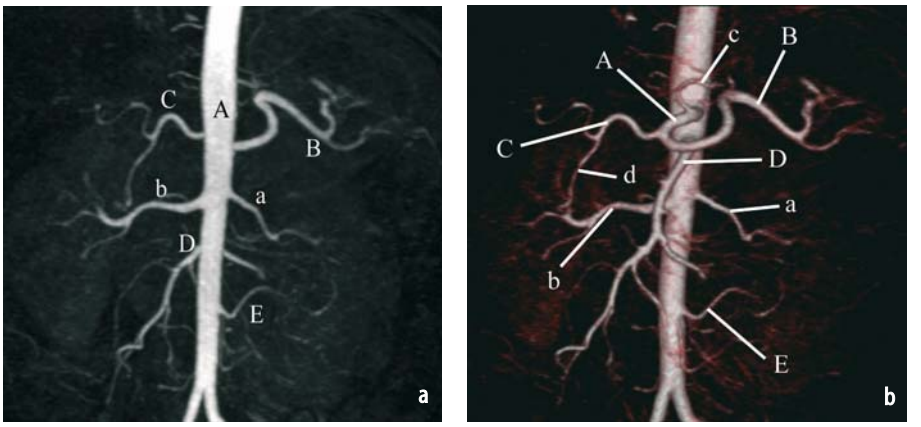

Fig. 1a, b. Maximum intensity projection (**a**) and volume rendered (**b**) displays of a 3D CE MRA dataset acquired in the early arterial phase demonstrate the arterial vascular anatomy of the abdomen. Beyond the aorta and both renal arteries, branches of the celiac trunk and the SMA are well-depicted.
A Celiac artery (CA). **B** Splenic artery. **C** Common hepatic artery. **D** Superior mesenteric artery (SMA). **E** Inferior mesenteric artery (IMA). **a** Left renal artery. **b** Right renal artery. **c** Left gastric artery. **d** Gastroduodenal artery.
From Magnetic Resonance Angiography, Schneider G. et al (eds.), p 233. Springer, 2005

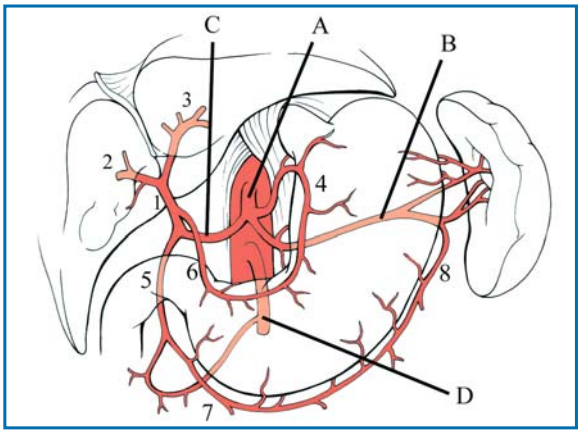

Fig. 2. Normal anatomy of the celiac trunk.
A Celiac artery (CA). **B** Splenic artery. **C** Common hepatic artery. **D** Superior mesenteric artery (SMA).
1 Proper hepatic artery. **2** Right hepatic artery. **3** Left hepatic artery. **4** Left gastric artery. **5** Gastroduodenal artery. **6** Right gastric artery. **7** Right gastroepiploic artery. **8** Left gastroepiploic artery.
From Magnetic Resonance Angiography, Schneider G. et al (eds.), p 232. Springer, 2005

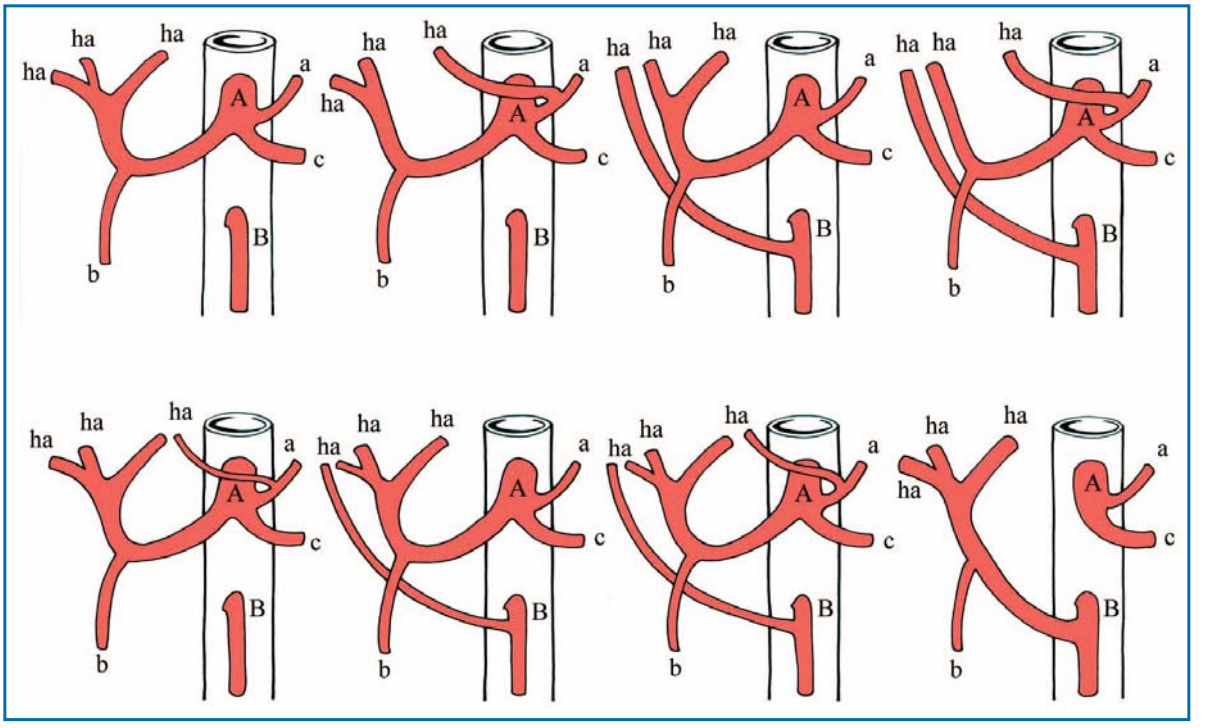

Fig. 3. Schematic representation of variants of the hepatic vasculature.
A Celiac artery (CA). **B** Superior mesenteric artery (SMA).
a Left gastric artery. **b** Gastroduodenal artery. **c** Splenic artery. **ha** Hepatic arteries
From Magnetic Resonance Angiography, Schneider G. et al (eds.), p 238. Springer, 2005

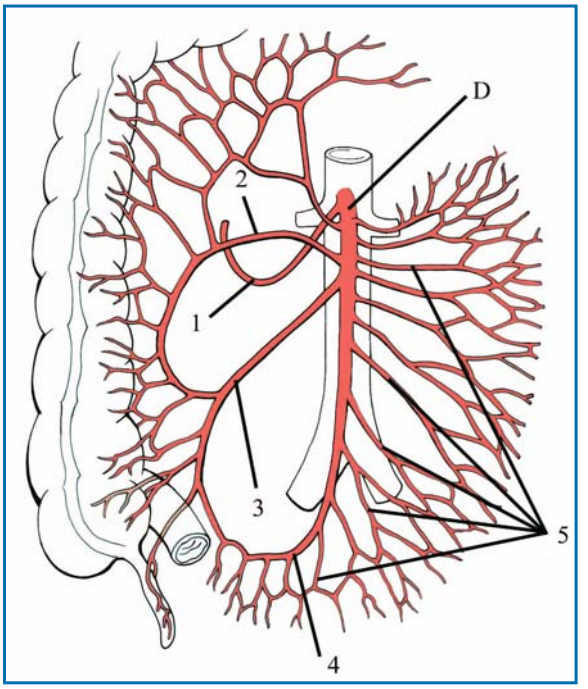

Fig. 4. Normal anatomy of the superior mesenteric artery.
D Superior mesenteric artery (SMA).
1 Gastroduodenal artery. **2** Medial colic artery. **3** Right colic artery. **4** Iliocolic artery. **5** Jejunal- and ilieal arteries.
From Magnetic Resonance Angiography, Schneider G. et al (eds.), p 232. Springer, 2005

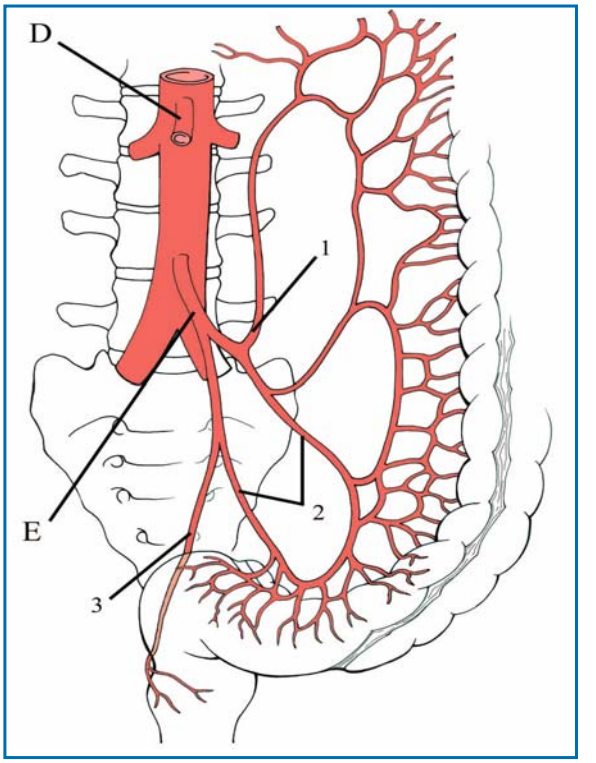

Fig. 5. Normal anatomy of the inferior mesenteric artery.
D Superior mesenteric artery (SMA). **E** Inferior mesenteric artery (IMA).
1 Left colic artery. **2** Sigmoid arteries. **3** Superior rectal artery.
From Magnetic Resonance Angiography, Schneider G. et al (eds.), p 232. Springer, 2005

it is a relatively thin vessel, measuring only 1-6 mm in diameter. For this reason the IMA is often difficult to depict on MRA.

The left colic artery usually represents the first branch of the IMA. This forms the so-called anastomosis of Riolan with the middle colic artery deriving from the SMA (Fig. 5). In cases of severe stenosis or occlusion of the SMA, this anastomosis can serve as a collateral supply for the SMA. Giving off the sigmoid branches, the IMA becomes the superior rectal artery.

Variations in the splanchnic arterial anatomy occur in more than 40% of patients (Fig. 3). For this reason, pre-operative vascular planning for hepatic resections, liver transplantations, resection of retroperitoneal masses, chemoinfusion pump placement, surgical shunting, or other abdominal operations may require accurate mapping of the visceral arterial anatomy. Generally, this is achieved by conventional angiography because of the fine detail needed to identify variations involving tiny arteries. However, to evaluate the origins of the splanchnic artery and major branches, 3D CE MRA is frequently sufficient.

The most common variation is a replaced (17%) or accessory (8%) right hepatic artery, most commonly from the SMA (Figs. 6, 7). Less common variations include the left hepatic artery arising from the left gastric artery (Fig. 8), the common hepatic artery arising from the SMA (2.5%) (Fig. 9) or directly from the aorta (2%) (Fig. 10), the left gastric artery arising from the aorta (1-2%) (Fig. 11), or a celio-mesenteric trunk (<1%). Other more complex variations may also occur.

Although the main indication for arterial imaging of the hepatic vasculature is the evaluation of vascular anatomy, there are other indications for which CE MRA may be helpful. For example, in the case of liver tumors such as pedunculated adenoma or focal nodular hyperplasia (FNH), preoperative CE MRA may help to optimize the therapeutic approach by displaying the arterial supply and venous drainage of the lesion (Fig. 12). Imaging of vascular pathologies such as aneurysms of the splanchnic arteries can also be performed in a non-invasive manner using CE MRA (Fig. 13) and therapeutic approaches, if necessary, can be planned.

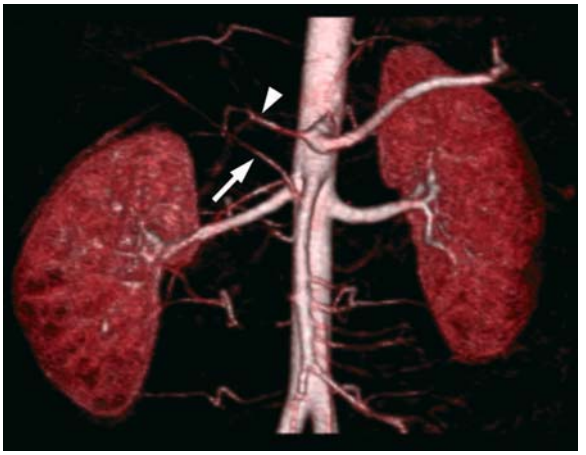

Fig. 6. A volume rendered 3D CE MRA (0.1 mmol/kg Gd-BOPTA) dataset shows an anatomic variation of the arterial supply of the liver in a patient with liver transplantation planned. Note that the right hepatic artery (*arrow*) branches from the SMA, whereas the left hepatic artery (*arrowhead*) branches from the celiac trunk. The small caliber of the vessels is the result of a longstanding inflammatory process that resulted in liver fibrosis

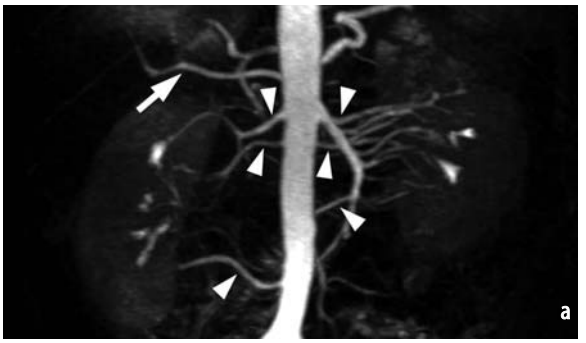

Fig. 7a, b. Whereas the MIP reconstruction (**a**) reveals multiple renal arteries (*arrowheads*) together with an obvious abnormal course of the right hepatic artery (*arrow*), the volume-rendered image (**b**) clearly displays the anatomic variation of a right hepatic artery originating from the SMA (*arrow*). This example shows that evaluation of vascular anatomy is sometimes easier on volume-rendered images than on MIP reconstructions

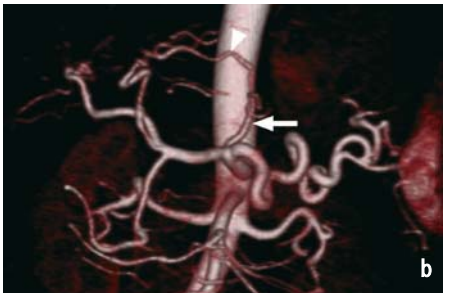

Fig. 8a, b. Left hepatic artery (*arrowhead*) arising from the left gastric artery (*arrow*) on a CE MRA (0.1 mmol/kg Gd-BOPTA) MIP reconstruction (**a**) and on a volume-rendered image (**b**). Note again that the vessels are better appreciated on the volume-rendered image

Fig. 9a, b. CE MRA in a 3 year old girl with transposition of the great arteries. Whole-body MIP reconstruction (**a**) reveals an abnormal course of the ascending aorta due to transposition of the great arteries and dextro-positio cordis. In addition, the splenic (arrowhead) and hepatic arteries (*arrow*) both seem to originate from the celiac trunk. However, a subvolume MIP reconstruction (**b**) clearly reveals that the common hepatic artery (*arrow*) branches from the SMA while the splenic artery (*arrowhead*) originates from the celiac trunk

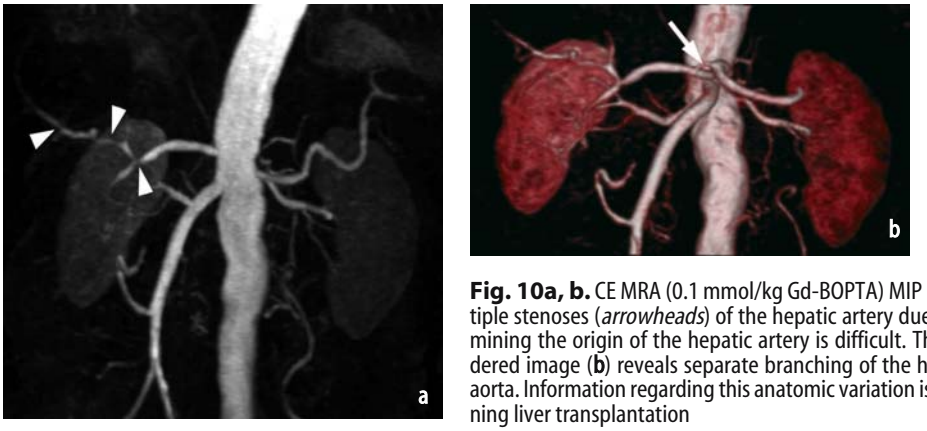

Fig. 10a, b. CE MRA (0.1 mmol/kg Gd-BOPTA) MIP reconstruction (**a**) reveals multiple stenoses (*arrowheads*) of the hepatic artery due to vasculitis. However, determining the origin of the hepatic artery is difficult. The corresponding volume-rendered image (**b**) reveals separate branching of the hepatic artery (*arrow*) from the aorta. Information regarding this anatomic variation is extremely important for planning liver transplantation

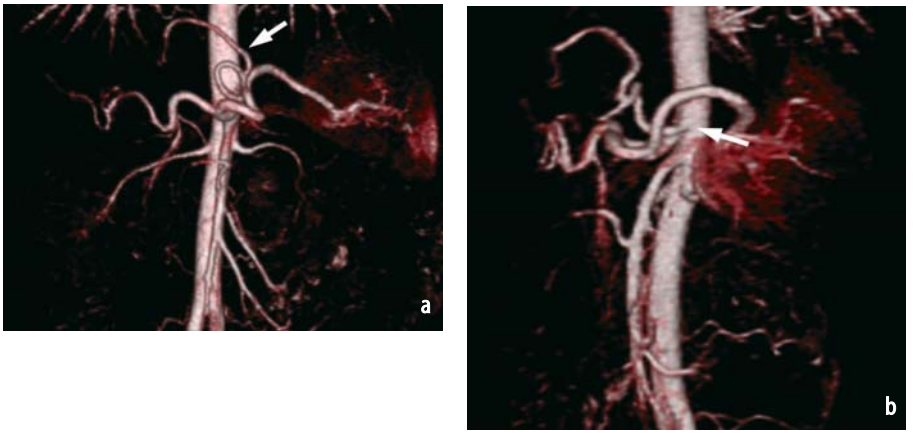

Fig. 11a, b. The volume-rendered image in AP-projection (**a**) demonstrates the left hepatic artery originating from the left gastric artery (*arrow*). The lateral view (**b**) reveals additional separate branching of the left gastric artery from the aorta (*arrow*)

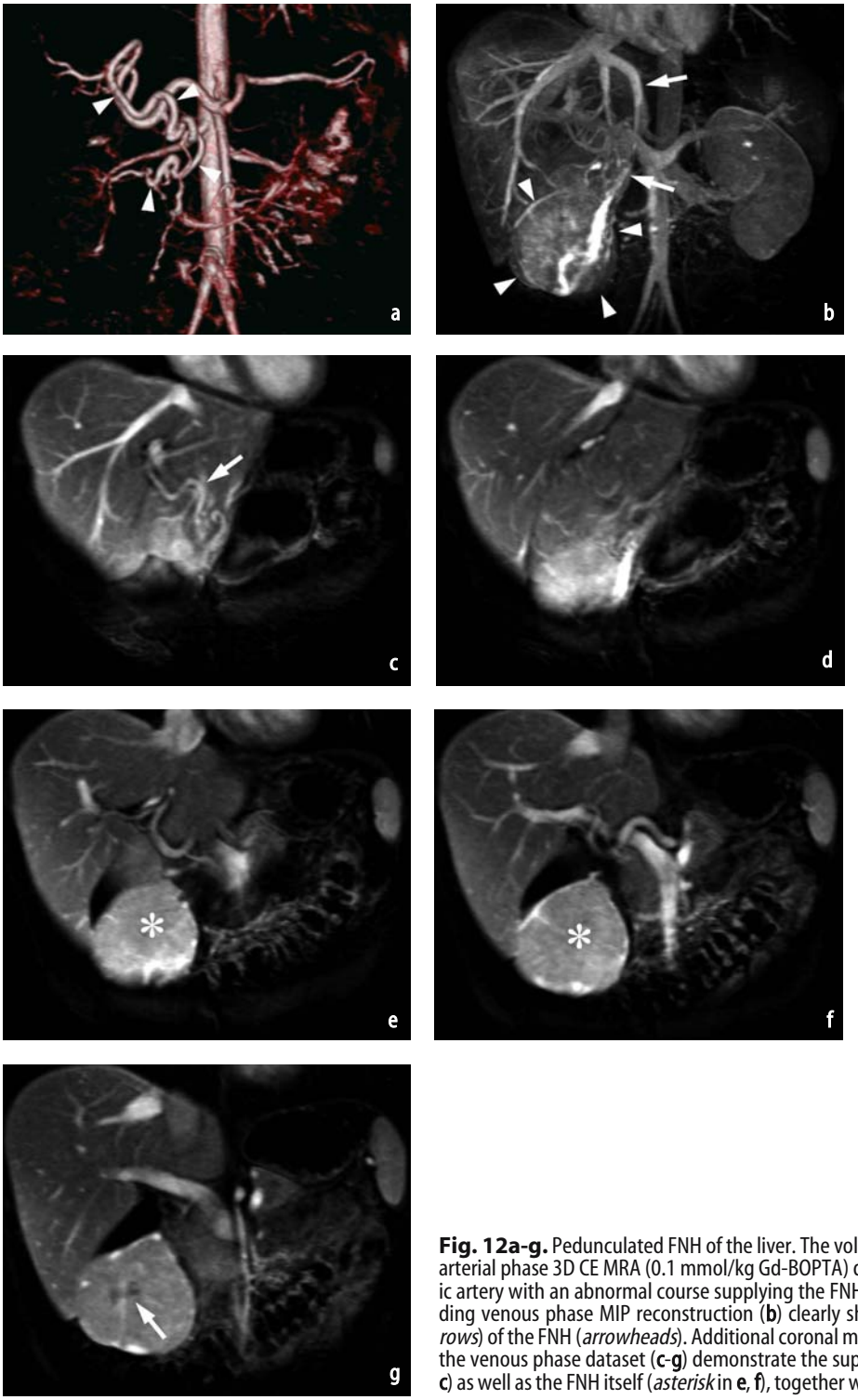

Fig. 12a-g. Pedunculated FNH of the liver. The volume-rendered image (**a**) of the arterial phase 3D CE MRA (0.1 mmol/kg Gd-BOPTA) dataset reveals a dilated hepatic artery with an abnormal course supplying the FNH (*arrowheads*). The corresponding venous phase MIP reconstruction (**b**) clearly shows the venous drainage (*arrows*) of the FNH (*arrowheads*). Additional coronal multiplanar reconstructions from the venous phase dataset (**c**-**g**) demonstrate the supplying hepatic artery (*arrow* in **c**) as well as the FNH itself (*asterisk* in **e**, **f**), together with the central scar (*arrow* in **g**)

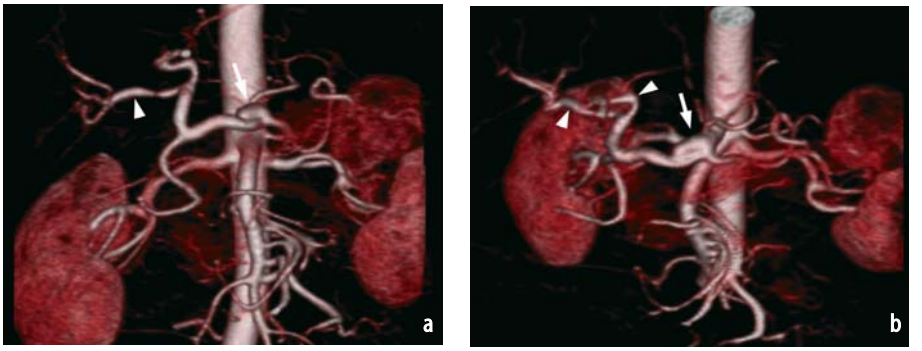

Fig. 13a, b. Volume-rendered images (**a**, **b**) in different orientations of a 3D CE MRA (0.1 mmol/kg Gd-BOPTA) dataset reveal multiple aneurysm formations in the celiac trunk (*arrow* in **b**) and hepatic arteries (*arrowheads*) due to systemic vascular disease

12.4 Imaging of the Portal-Venous System

3D CE MR portography is regarded as a safe, quick and robust imaging modality for evaluation of the portal-venous system. This technique has been shown to be advantageous compared to currently used techniques such as ultrasonography, catheter angiography, computed tomography (CT), and non-enhanced MR angiography with TOF and phase contrast (PC) techniques [22].

There are no major differences between MRA of the abdominal arterial system and MR portography in terms of patient management, coil selection and MR sequences. After acquisition of a precontrast coronal 3D gradient echo dataset, contrast agent is injected and image acquisition commences. Typically, image acquisition on MR portography is timed to the arterial vessel system with an additional acquisition delay of 40-60 sec after contrast agent injection prior to acquisition of the portal-venous dataset. At post-processing, the precontrast and CE arterial phase datasets are subtracted from the portal-venous phase dataset to enable visualization of the portal-venous system without arterial overlay. MIP reconstruction and multiplanar reformation techniques permit accurate evaluation of the portal-venous system.

The simultaneous availability of coronal source images permits demonstration of parenchymal lesions of the liver, pancreas, biliary tract and spleen. Precise and reliable assessment of the portal-venous system in patients with hepatic cirrhosis and portal hypertension is essential before liver transplantation, non-surgical transjugular shunting or surgical portosystemic shunting. In patients with portal hypertension and a history of gastroesophageal bleeding, it is mandatory to ascertain whether the portal-venous system is patent or if the portal vein or its main branches are thrombosed [28].

12.4.1 Normal Anatomy and Variants

The portal vein represents a confluence of the superior mesenteric vein (SMV) and the main splenic vein into which drains the pancreatic vein, left gastroepiploic vein, short gastric vein, and inferior mesenteric vein (IMV) (Fig. 14). The IMV receives its supply from the left colic, sigmoid and superior hemorrhoidal veins. It usually joins the splenic vein prior to the junction of the splenic vein with the SMV. The SMV receives its contribution from the jejunal, ileal, right colic, and middle colic veins. The right and left gastric veins usually drain directly into the portal vein.

The portal vein then divides into the right and left portal branches at the hepatic hilum. Approximately 50% of individuals demonstrate a bifurcation of the portal vein outside the liver capsule. A common anomaly of the portal-venous system is a trifurcation of the main portal vein, which occurs in about 8% of patients. In this case, the main portal vein divides into the right posterior segmental branch, the right anterior segmental branch and the left portal vein [11, 19].

12.4.2 Clinical Implications

3D CE MR portography permits accurate evaluation of the intra- and extrahepatic portal-venous system as well as the hepatic veins (Fig. 15). Due to the large field of view, the short time of acquisition, the lack of radiation, the non-invasive nature of the procedure and the low risk of complications, MR portography is regarded as superior to conventional catheter digital subtraction angiography (DSA). Clinical applications of 3D CE MR portography include the assessment of portal hypertension (portosystemic shunt, portal vein obstruction, hepatic vein obstruc-

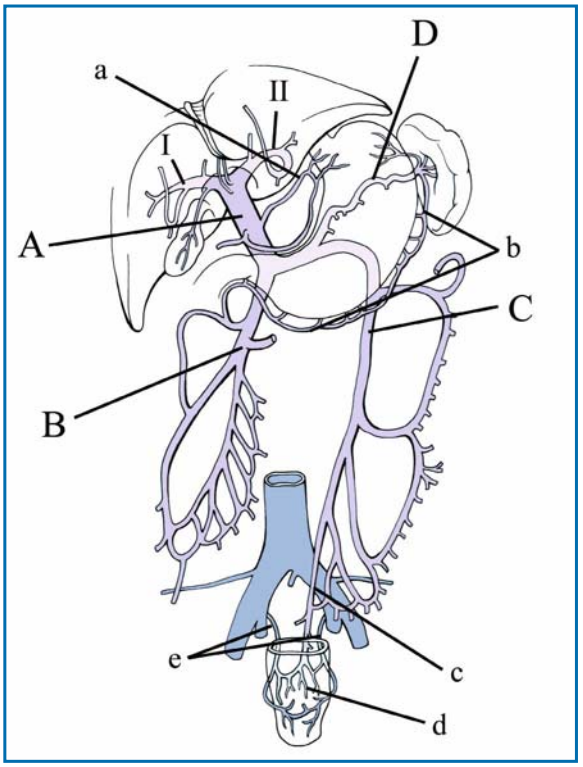

Fig. 14. Normal anatomy of the portal-venous system.
A Portal vein. **B** Superior mesenteric vein (SMV). **C** Inferior mesenteric vein (IMV). **D** Lienal (splenic) vein.
I Right branch of the portal vein. **II** Left branch of the portal vein.
a Coronary and pyloric veins. **b** Right and left gastroepiploic veins.
c Superior hemorrhoidal vein. **d** Hemorrhoidal plexus. **e** Middle and inferior hemorrhoidal veins. From Magnetic Resonance Angiography, Schneider G. et al (eds.), p 243. Springer, 2005

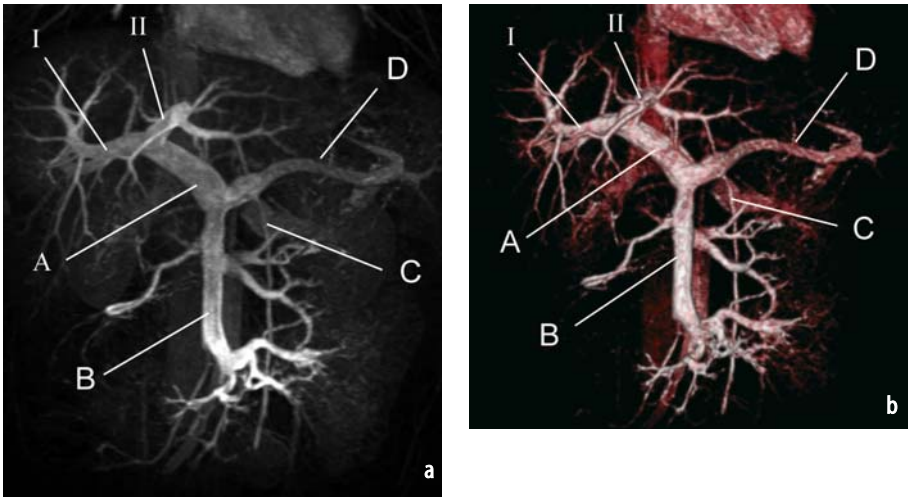

Fig. 15a, b. Normal anatomy of the portal-venous system on CE MRA MIP reconstruction (**a**) and volume-rendered image (**b**).
A Portal vein. **B** Superior mesenteric vein (SMV). **C** Inferior mesenteric vein (IMV). **D** Lienal (splenic) vein.
I Right branch of the portal vein. **II** Left branch of the portal vein

tion), hepatic encephalopathy, ascending portal thrombophlebitis, hepatocellular carcinoma (HCC) and pancreatobiliary tumors, gastrointestinal hemorrhage, and differentiation of splanchnic arterial disease from portal-venous disease [22, 33].

In patients with portal hypertension, 3D MR portography can be used to evaluate portosystemic shunts, hepatorenal collateral pathways, and obstruction of the portal or hepatic veins. In planning treatment for hepatic encephalopathy, it is important to identify the causative portosystemic shunt. In suspected cases of ascending portal thrombophlebitis, it is important to assess the severity of portal vein obstruction as well as portal collateral vessels. In patients with HCC or pancreatobiliary tumors, the presence or absence of portal vein invasion should be determined when planning treatment.

12.4.3 Evaluation in Liver Transplantation

Imaging proof of a patent portal vein is required in order for a patient to be placed on the liver transplant waiting list. Ultrasound (US) can image the portal vein, but is not 100% reliable. When US fails to adequately visualize the portal vein, 3D CE MRA offers a safe, accurate, and comprehensive assessment of portal-venous anatomy without requiring iodinated contrast medium [10, 12]. 3D CE MRA is also able to evaluate the splenic vein, SMV, IMV, inferior caval vein (ICV) and potential varices. Following liver transplantation, rising liver function tests may raise a suspicion of allograft ischemia. Since blood supply to the liver occurs primarily via the portal vein, this is the most important vessel to evaluate. The most common site of obstruction is at the anastomosis. Usually, anastomoses are easy to identify because of the caliber change between donor and recipient portal veins [23]. Stenosis of the transplant arterial anastomosis may be seen on the arterial phase of a portal-venous study, but its smaller size and often folded, tortuous course can make it difficult to assess. Occlusion of the transplant artery is important to detect because it results in ischemia to the donor common bile duct and can lead to biliary strictures and leaks. It is also important to assess the ICV since supra- and infrahepatic ICV anastomoses may also become narrowed and flow limiting.

12.4.4 Portal Vein Thrombosis and Cavernous Transformation

Thrombosis of the portal vein is a pathology that is frequently found in liver cirrhosis, pancreatitis, ascending portal thrombophlebitis or after sclerotherapy of a gastroesophageal varix [1]. In this condition it is important to acquire accurate information regarding portal-venous patency (Fig. 16). 3D CE MR portography provides detailed information not only about the location and length of portal vein obstruction, but also about portal collateral pathways (Fig. 17). Over time, a network of small collateral vessels develops to bypass the portal-venous occlusion. This network of collaterals, known as a cavernous transformation, is identified by its characteristic enhancement pattern in the hepatic hilum during the portal-venous and equilibrium phases of imaging (Fig. 18).

While color Doppler ultrasonography often fails to evaluate portal venous patency, 3D CE MR portography usually provides accurate information [7]. Furthermore, CE MRA can be used to assess surgical portosystemic shunts which are frequently placed to reduce portal-venous pressure. In this scenario CE MRA is used to evaluate the patency of the shunt (Fig. 19) and possible complications such as stenosis at the anastomosis.

12.4.5 Tumor Encasement

In patients with pancreatobiliary tumors, it is important to evaluate portal vein invasion before surgery. Whereas CT and DSA are often used for this purpose, 3D CE MR portography is also an accurate means to diagnose portal vein invasion [16, 30]. Invasion of the portal vein makes tumor resection with clear margins nearly impossible, thus removing the patient as a surgical candidate. Tumors in the pancreatic head may encase the SMV, portal vein, and medial splenic vein. Because these tumors cause biliary obstruction, they are usually detected quickly and are therefore more often resectable. Tumors in the body and tail of the pancreas cause less biliary obstruction and therefore frequently become larger before being detected. These tumors commonly occlude the splenic vein. Splenic vein occlusion has a tendency to produce short gastric varices which serve as venous collaterals. These can usually be seen on delayed images.


a


b

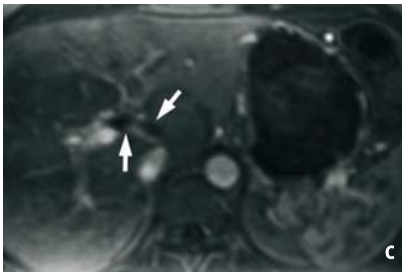
c

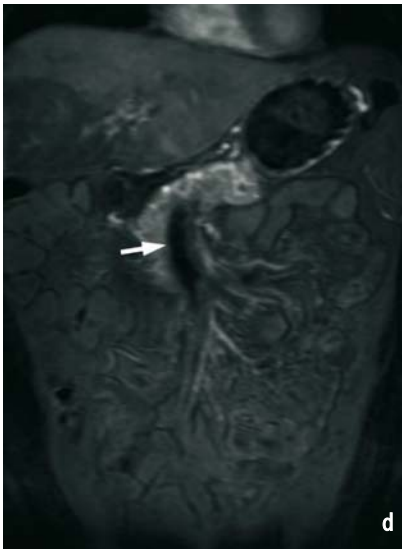
d

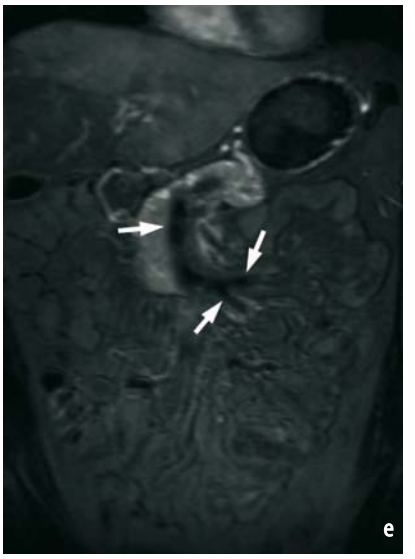
e

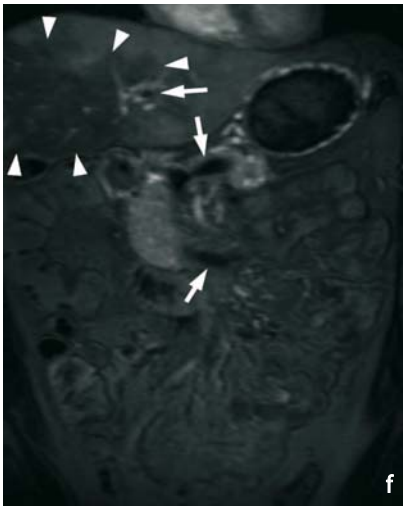
f

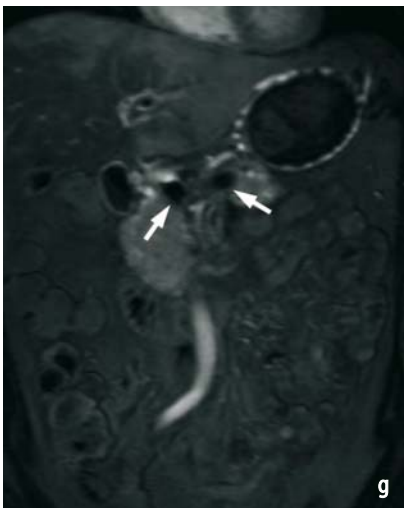
g

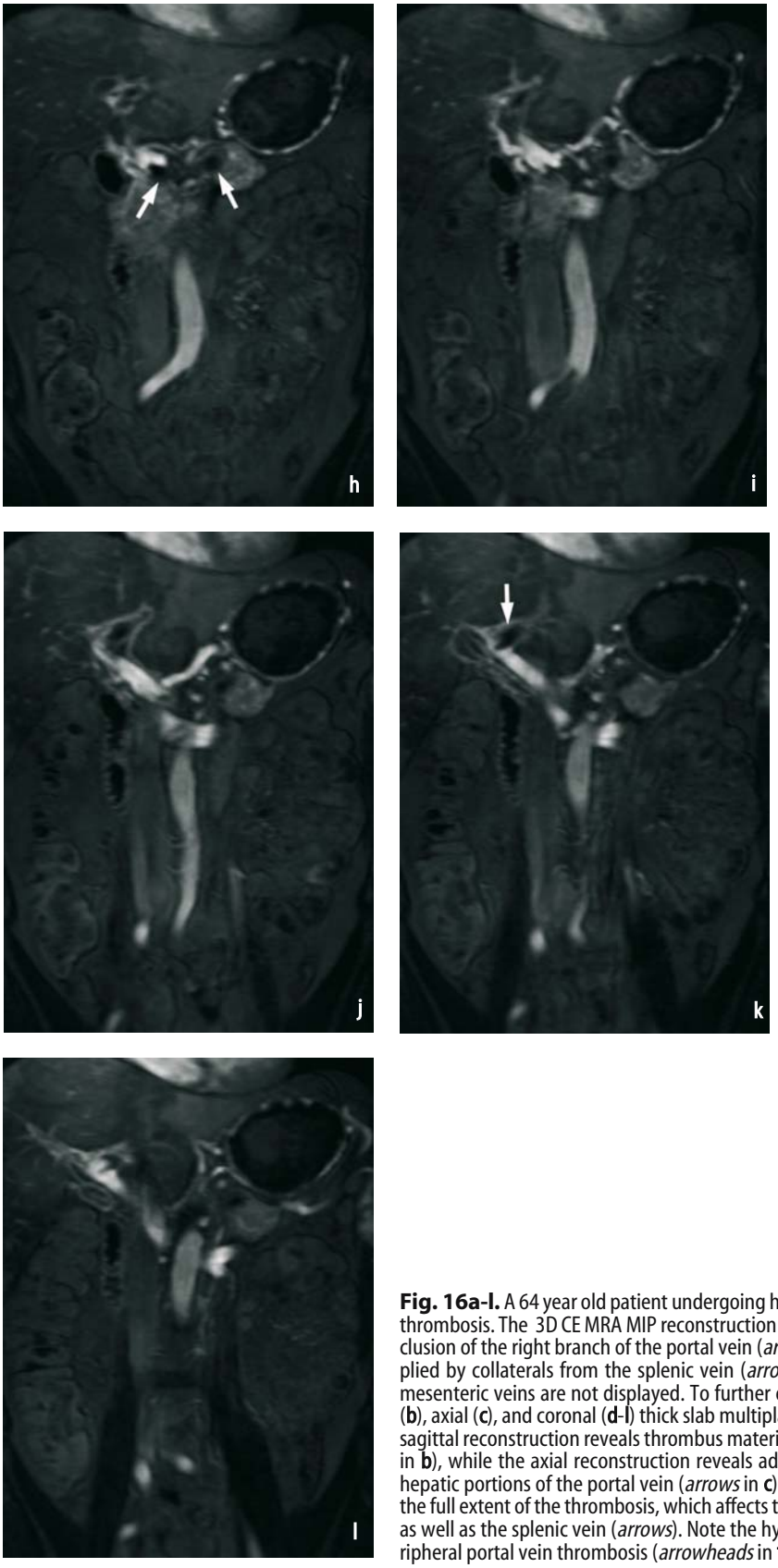

Fig. 16a-l. A 64 year old patient undergoing high dose chemotherapy, with portal vein thrombosis. The 3D CE MRA MIP reconstruction (**a**) in the portal-venous phase shows occlusion of the right branch of the portal vein (*arrows*). In addition, the portal vein is supplied by collaterals from the splenic vein (*arrowhead*), while the superior and inferior mesenteric veins are not displayed. To further evaluate the anatomic situation, sagittal (**b**), axial (**c**), and coronal (**d**-**l**) thick slab multiplanar reconstructions were prepared. The sagittal reconstruction reveals thrombus material in the superior mesenteric vein (*arrow* in **b**), while the axial reconstruction reveals additional thrombus material in the intrahepatic portions of the portal vein (*arrows* in **c**). The coronal reconstructions (**d**-**l**) reveal the full extent of the thrombosis, which affects the superior and inferior mesenteric veins as well as the splenic vein (*arrows*). Note the hypoperfusion of hepatic tissue due to peripheral portal vein thrombosis (*arrowheads* in **f**)

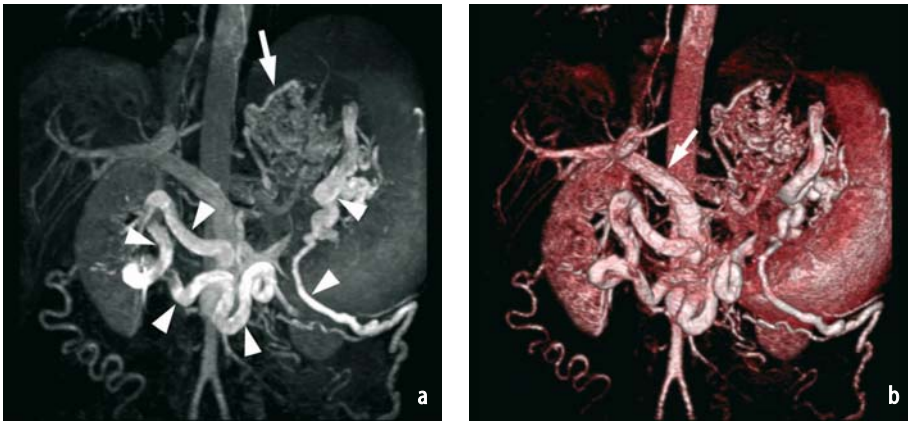

Fig. 17a, b. Extensive collateral mesenteric vessels in a patient after splenic vein thrombosis due to pancreatitis. Imaging was performed to rule out portal vein thrombosis.
The 3D CE MRA (0.1 mmol/kg Gd-BOPTA) MIP reconstruction (**a**) reveals an extensive number of collateral vessels (*arrow*) in the area of the gastric veins. In addition, collateral vessels (*arrowheads*) that drain blood from the splenic hilum to the abdominal wall and into the superior mesenteric vein are also visible. However, both the MIP reconstruction (**a**) and the volume-rendered image (**b**) reveal a patent portal vein with normal intrahepatic branching (*arrow* in **b**)

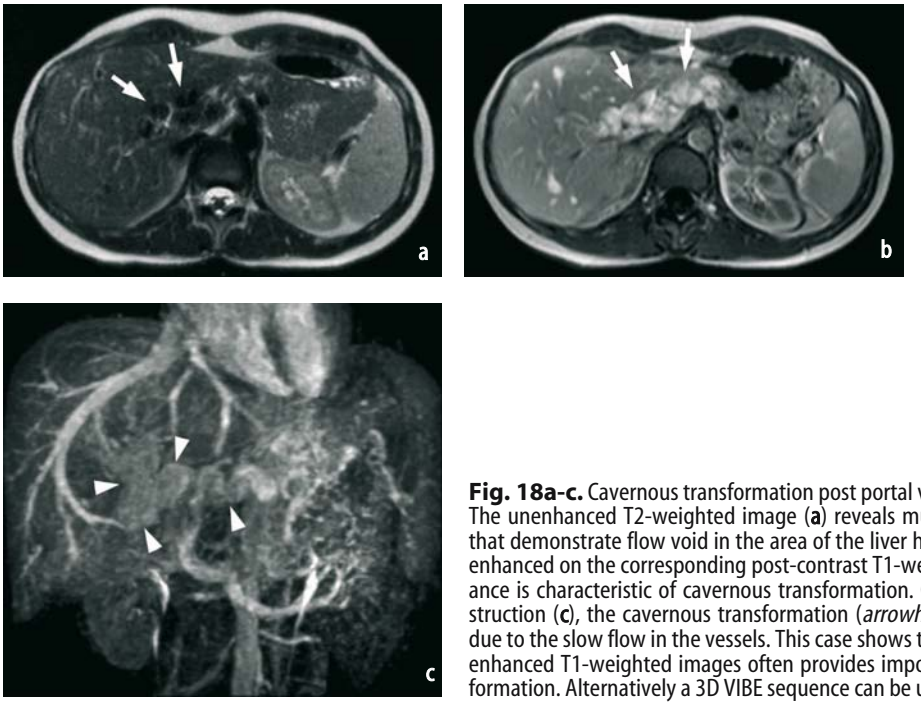

Fig. 18a-c. Cavernous transformation post portal vein occlusion.
The unenhanced T2-weighted image (**a**) reveals multiple dilated vessels (*arrows*) that demonstrate flow void in the area of the liver hilum. The vessels are markedly enhanced on the corresponding post-contrast T1-weighted image (**b**). This appearance is characteristic of cavernous transformation. On the 3D CE MRA MIP reconstruction (**c**), the cavernous transformation (*arrowheads*) is only faintly enhanced due to the slow flow in the vessels. This case shows that the acquisition of contrast-enhanced T1-weighted images often provides important additional diagnostic information. Alternatively a 3D VIBE sequence can be utilized

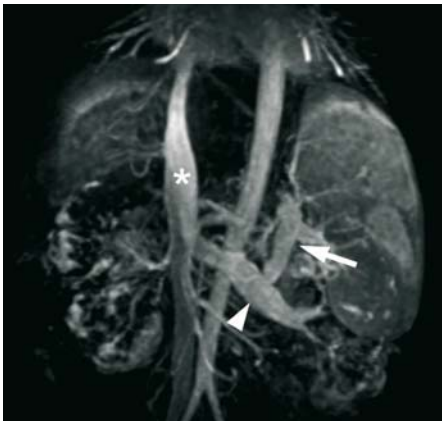

Fig. 19. Patent surgical spleno-renal shunt performed for lowering portal hypertension in a patient with liver fibrosis and recurrent bleeding from esophageal varices.
The 3D CE MRA study reveals a patent spleno-renal shunt with clear depiction of the vein graft (*arrow*), the left renal vein (*arrowhead*) and the ICV (*asterisk*)

12.5 Imaging of the Venous System

12.5.1 Normal Anatomy and Variants

The systemic venous architecture of the liver comprises three main venous vessels which drain into the ICV: the right hepatic vein, the middle hepatic vein and the left hepatic vein. In about 60% of individuals, the left hepatic vein and the middle hepatic vein form a common trunk which drains separately into the ICV. Normally, the right hepatic vein drains liver segments V-VII, the middle hepatic vein drains segments IV, V and VIII, and the left hepatic vein drains segments II and III. Venous drainage from segment I usually occurs directly into the ICV. This is considered the cause of hypertrophy of this segment in cirrhotic livers as result of an improved blood supply [13, 31].

12.5.2 Budd-Chiari Syndrome / Veno-Occlusive Disease

Budd-Chiari syndrome is a disorder characterized by hepatic outflow occlusion which has a variety of causes [9, 32]. In planning treatment, it is important to determine the location and length of hepatic outflow obstruction [20], and 3D CE MR portovenography is an accurate means of achieving this.

Heptatic outflow is also occluded in veno-occlusive disease. However, since it is the small intrahepatic veins that are affected in this disease, imaging findings frequently reveal larger liver veins that may have decreased calibre but which are nevertheless still patent.

Further details about these diseases and imaging examples can be found in Chapter 9, "Imaging of Diffuse Liver Disease".

12.6 Evaluation of Living Donors in Liver Transplantation

Resection of the liver from living donors for transplantation is a special surgical challenge. The success of the surgical procedure depends heavily on preoperative planning for which knowledge of the hepatic vasculature, as well as of the presence of hepatic neoplasms and their relationship to adjacent vessels, is crucial.

Conventional catheter angiography has long been considered the "gold standard" technique for evaluation of hepatic arterial anatomy. However, the morbidity and mortality associated with catheter angiography, coupled with the limitations of this procedure in demonstrating the hepatic venous anatomy, have provided impetus for the development of non-invasive methods [29]. Nowadays, CE MRA is increasingly considered a superior imaging modality for evaluating the hepatic vessels. Comprehensive information concerning the hepatic parenchyma as well as the complex arterial, venous and portal venous systems can today be obtained using a "one-stop-shop" examination.

Special care has to be taken when planning liver resection for living donor transplantation. As the rate of vascular abnormalities is comparatively high in the liver, accurate depiction of the arterial, venous and portal venous systems is important for successful resection of the graft as well as for replantation into the host. Knowledge of the relationship between intrahepatic neoplasms and adjacent vessels is also crucial for planning resection with tumor-free margins.

12.7 Segmental Anatomy of the Liver

The segmental anatomy of the liver is based on the vascular supply and drainage of the parenchyma. Until recently, classification of the liver lobes and sub-segments in the international literature was not uniform. Whereas British and American publications tended to follow the terminology of Goldsmith and Woodburne [8], in Europe and Japan the most common nomenclature used by radiologists and surgeons was based on the description of Couinaud and Bismuth [3, 5]. According to the terminology of Goldsmith and Woodburne [8], the liver comprises two liver lobes (left and right) separated by the middle hepatic vein, and four segments. While the right liver lobe consists of the right anterior and right posterior segments separated by the right hepatic vein, the left lobe is subdivided into the left medial and left lateral segments separated by the left hepatic vein.

Conversely, the classification of Couinaud and Bismuth [3, 5] describes a liver that is divided into a left and a right liver or hemiliver and sub-divided into four sectors and eight segments. Each of these eight segments is independent in terms of blood supply and biliary drainage. This allows for individual resection of a given segment without harm or alteration to the circulation of the remaining liver parenchyma. The left and right liver according to Couinaud and Bismuth correspond directly to the hepatic lobes described by Goldsmith and Woodburne [8]. The right hemiliver is further subdivided into a right paramedian sector and a right lateral sector consisting of two anterior

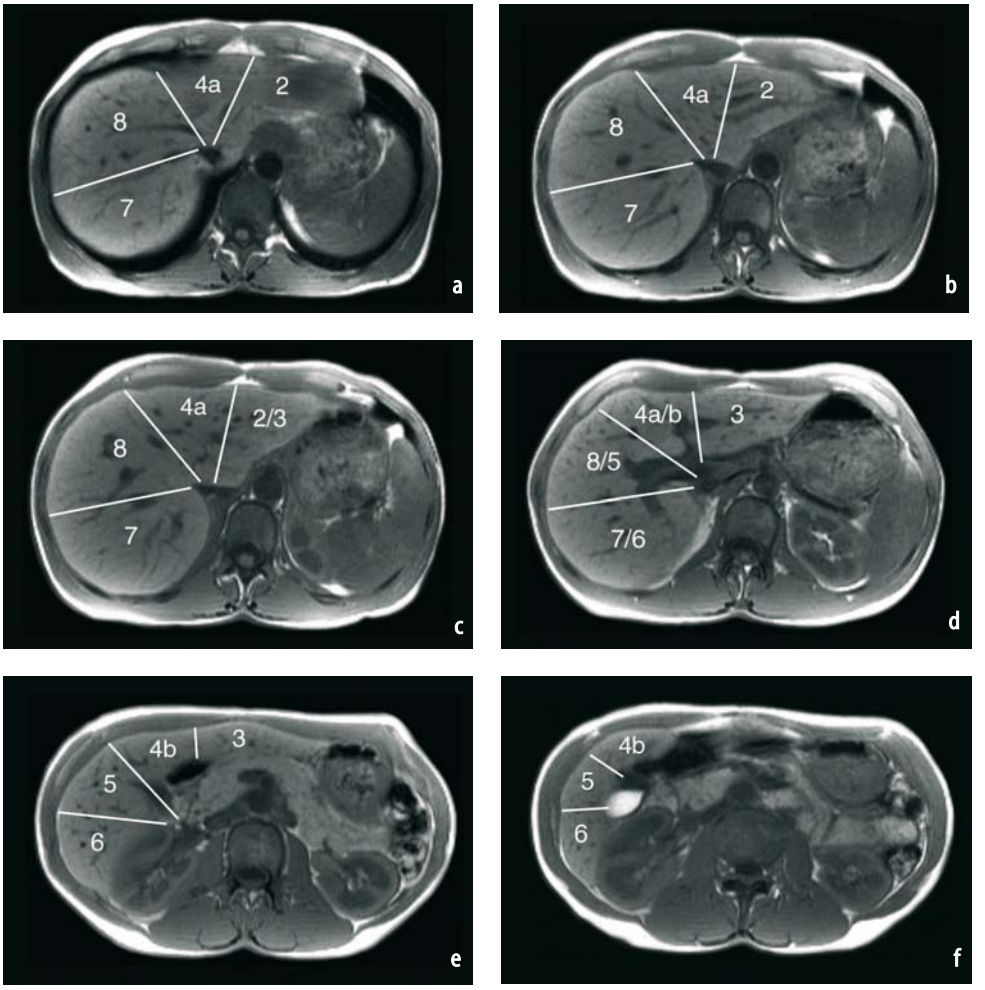

Fig. 20a-f. Segmental anatomy of the liver according to Couinaud and Bismuth

inferior and two posterior superior segments, respectively. Similarly, the left hemiliver comprises a left paramedian sector and a left lateral sector which are further sub-divided into anterior inferior and posterior superior segments.

The eight liver segments described by Couinaud and Bismuth [3, 5] are numbered clockwise based on a frontal view of the liver beginning with the posterior superior segment of the left paramedian sector, which corresponds to the caudate lobe, and ending with segment VIII which is consistent with the posterior superior segment of the right paramedian sector [6]. Today, the most common classification of liver segments is based on the Couinaud and Bismuth classification [3, 5].

Anatomically, the borders of the liver segments are well-defined, but show a wavy-shaped course [24]. However, in clinical routine, segmentation of the liver on cross-sectional CT and MR imaging is sharply demarcated and usually based on certain landmarks that define the underlying borders (Fig. 20). Based on these landmarks, the ICV is considered the center point for liver segmentation. A line from the ICV to the middle hepatic vein and the gallbladder separates the left and right hemilivers and the corresponding liver segments V/VIII and I/IVa, b, respectively. Whereas the axis between the ICV and right hepatic vein corresponds to the border between liver segments VI/VII and V/VIII, the line between the ICV, the left hepatic vein and the falciform ligament separates liver segments IVa and IVb from segments II and III.

Whereas liver segments VII, VIII, I, IVa and II are located at the posterior aspect of the imaged abdominal situs and above the level of the left and right main portal vein, segments VI, V, IVb and III are located inferior to the level of the main portal veins at the anterior aspect of the liver. Segment I corresponds to the caudate lobe.

References

1. Abbitt PL. Portal vein thrombosis: imaging features and associated etiologies. Curr Probl Diagn Radiol 1992;21:115-147
2. Baden JG, Racy DJ, Grist TM. Contrast-enhanced three-dimensional magnetic resonance angiography of the mesenteric vasculature. J Magn Reson Imaging 1999;10:369-375
3. Bismuth H. Surgical Anatomy and Anatomical Surgery of the Liver. World J Surg 1982;6:3-9
4. Burkart DJ, Johnson CD, Reading CC, et al. MR measurements of mesenteric venous flow: prospective evaluation in healthy volunteers and patients with chronic mesenteric ischemia. Radiology 1995; 194:801-806
5. Couinaud C. Le Foie. Etudes anatomiques et chirurgicales. Paris, Masson & Cie, 1957
6. Fasel JH, Gailloud P, Terrier F, Mentha G, Sprumont P. Segmental anatomy of the liver: a review and a proposal for an international working nomenclature. Eur Radiol 1996;6:834-7
7. Glassman MS, Klein SA, Spivak W. Evaluation of cavernous transformation of the portal vein by magnetic resonance imaging. Clin Pediatr 1993;32:77-80
8. Goldsmith NA, Woodburne RT. The surgical anatomy pertaining to liver resection. Surg Gynecol Obstet 1957;105(3):310-8
9. Gore RM. Vascular disorders of the liver and splanchnic circulation. In: Gore RM, Levine MS, Laufer I (eds). Textbook of gastrointestinal radiology. Saunders, Philadelphia 1994, 2018-2050
10. Goyen M, Barkhausen J, Debatin JF, Kuhl H, Bosk S, Testa G, Malago M, Ruehm SG. Right-lobe living related liver transplantation: evaluation of a comprehensive magnetic resonance imaging protocol for assessing potential donors. Liver Transpl 2002; 8:241-250
11. Hagspiel KD, Leung DA, Angle JF, Spinosa DJ, Pao DG, de Lange EE, Butty S, Matsumoto AH. MR angiography of the mesenteric vasculature. Radiol Clin North Am 2002;40:867-886
12. Lee VS, Morgan GR, Teperman LW, John D, Diflo T, Pandharipande PV, Berman PM, Lavelle MT, Krinsky GA, Rofsky NM, Schlossberg P, Weinreb JC. MR imaging as the sole preoperative imaging modality for right hepatectomy: a prospective study of living adult-to-adult liver donor candidates. Am J Roentgenol 2001;176:1475-1482
13. Lerut JP, Mazza D, van Leeuw V, Laterre PF, Donataccio M, de Ville de Goyet J, Van Beers B, Bourlier P, Goffette P, Puttemans T, Otte JB. Adult liver transplantation and abnormalities of splanchnic veins: experience in 53 patients. Transpl Int 1997;10:125-132
14. Li KCP, Hopkins KL, Dalman RL, et al. Simultaneous flow measurements within the superior mesenteric vein and artery with cine phase-contrast MR imaging: value in diagnosis of chronic mesenteric ischemia. Radiology 1995;194:327-330
15. Li KCP, Whitney WS, McDonnell C, et al. Chronic mesenteric ischemia: evaluation with phase-contrast cine MR imaging. Radiology 1994;190:175-179
16. McFarland EG, Kaufman JA, Saini S, Halpern EF, Lu DS, Waltman AC, Warshaw AL. Pre-operative staging of cancer of the pancreas: value of MR angiography versus conventional angiography in detecting portal venous invasion. Am J Roentgenol 1996;166:37-43
17. Meaney JF. Non-invasive evaluation of the visceral arteries with magnetic resonance angiography. Eur Radiol 1999;9:1267-1276
18. Meaney JFM, Prince MR, Nostrand TT, et al. Gadolinium-enhanced magnetic resonance angiography in patients with suspected chronic mesenteric ischemia. J Magn Reson Imaging 1997;7:171-176
19. Michels NA. Blood supply and anatomy of the upper abdominal organs. JB Lipincott Co, Philadelphia 1955
20. Murphy FB, Steinberg HV, Shires GT 3rd, Martin LG, Bernardino ME. The Budd-Chiari syndrome: a review. AM J Roentgenol 1986;147:9-15
21. Naganawa S, Cooper TG, Jenner G, et al. Flow velocity and flow measurement of superior and inferior mesenteric artery with cine phase contrast magnetic resonance angiography. Radiat Med 1994;12:213-220
22. Okumura A, Watanabe Y, Dohke M, Ishimori T, Amoh Y, Oda K, Dodo Y. Contrast-enhanced three-dimensional MR portography. Radiographics 1999 Jul-Aug;19(4):973-87
23. Pandharipande PV, Lee VS, Morgan GR, Teperman LW, Krinsky GA, Rofsky NM, Roy MC, Weinreb JC. Vascular and extravascular complications of liver transplantation: comprehensive evaluation with three-dimensional contrast-enhanced volumetric MR imaging and MR cholangiopancreatography. Am J Roentgenol 2001;177:1101-1107
24. Platzer W, Maurer H. On the segmental arrangement of the liver. Acta Anat (Basel) 1966;63:8-31
25. Prince MR, Grist TM, Debatin JF. Mesenteric Arteries. In: Prince MR, Grist TM, Debatin JF. 3D Contrast MR Angiography. Springer, Berlin, Heidelberg, New York 2003
26. Prince MR, Narasimham DL, Stanley JC, et al. Breathhold gadolinium-enhanced MR arteriography of the abdominal aorta and its major branches. Radiology 1995;197:785-792
27. Prince MR, Yucel EK, Kaufman JA, et al. Dynamic gadolinium-enhanced 3D abdominal MR arteriography. J Magn Reson Imaging 1993;3:877-881
28. Redvanly RD, Nelson RC, Stieber AC, Dodd GD 3rd. Imaging in the preoperative evaluation of adult liver-transplant candidates: goals, merits of various procedures, and recommendations. Am J Roentgenol 1995;164:611-617
29. Sahani D, Mehta A, Blake M, Prasad S, Harris G, Saini S. Preoperative Hepatic Vascular Evaluation with CT and MR Angiography: Implications for Surgery. Radiographics 2004;24:1367–1380
30. Smedby O, Riesenfeld V, Karlson B, Jacobson G, Lofberg A, Lindgren PG, Ahlstrom H. Magnetic resonance angiography in the resectability assessment of suspected pancreatic tumors. Eur Radiol 1997;7:649-653
31. Soyer P, Heath D, Bluemke DA, Choti MA, Kuhlman JE, Reichle R, Fishman EK. Three-dimensional helical CT of intrahepatic venous structures: comparison of three rendering techniques. J Comput Assist Tomogr 1996;20:122–127
32. Spritzer CE. Vascular disease and MR angiography of the liver. Magn Reson Imaging Clin N Am 1997;5:377-396
33. Vosshenrich R, Fischer U. Contrast-enhanced MR angiography of abdominal vessels: is there still a role for angiography? Eur Radiol 2002;12:218-230
34. Wasser MN, Geelkerken RH, Kouwenhoven M, et al. Systolically gated phase-contrast MRA of mesenteric arteries in suspected mesenteric ischemia. J Comput Assist Tomogr 1996;20:262-268